INTERNATIONAL JOURNAL FOR NUMERICAL METHODS IN FLUIDS, VOL. 25, 1043–1056 (1997)

NUMERICAL SIMULATION OF THE GROUND EFFECT USING THE BOUNDARY ELEMENT METHOD

KATSUHIRO KIKUCHI,* FUMINORI MOTOE AND MITSUNORI YANAGIZAWA

Department of Physics, Science University of Tokyo, 1–3 Kagurazaka, Shinjuku-ku, Tokyo 162, Japan

SUMMARY

As is well known, the lift of a wing passing over the ground becomes larger than that of a wing in a finite air field because of the ground effect. Owing to its special aerodynamic characteristics and applications, the problem of the ground effect has become increasingly common. In this paper some investigations were conducted to calculate the unsteady aerodynamic forces for long and short ground plates by means of boundary element techniques. In order to calculate the pressure variation on a long ground plate, the steady boundary element method was used. However, when using a short ground plate, the boundary element method was modified to treat the unsteady aerodynamic phenomena. Experimental studies were also made for both ground plates to confirm the validity of the numerical results. At low angles of attack the qualitative behaviour of the unsteady aerodynamic pressure on both ground plates was well predicted by the boundary element methods and qualitative agreement is found between the calculated and measured results. © 1997 John Wiley & Sons, Ltd.

Int. J. Numer. Meth. Fluids, **25**: 1043–1056 (1997)

No. of Figures: 17. No. of Tables: 0. No. of References: 14.

KEY WORDS: ground effect; boundary element method; unsteady aerodynamic force; relative motion

1. INTRODUCTION

As an aerodynamic feature of an aircraft, it is pointed out that an aircraft flying very near the ground (usually the surface of a runway) is apt to be influenced by the ground when the flying body is landing on or taking off from the runway. The change in flight characteristics of the aircraft due to the ground is widely known as the ground effect.[1] The study of ground effect wings for which the said ground effect is positively utilized has been made in a wide range of research fields.[2–5]

Since performance of computers has lately been remarkably enhanced and dependence on computational fluid dynamics has also been increased, problems concerning the ground effect are being vigorously solved. However, when this matter is to be dealt with by the finite difference method, fault is found owing to a variety of conditions, with the result that unacceptably long time and enormous expense are required for the calculation of just one case even with today's high-performance computers.

The singularity method or panel method is a method taking linear approximation as a premise and can be said to be the optimum method for aerodynamic characteristic prediction by virtue of its

* Correspondence to: K. Kikuchi, Yanagizawa Laboratory, Department of Physics, Science University of Tokyo, 1–3 Kagurazaka, Shinjuku-ku, Tokyo 162, Japan.

CCC 0271–2091/97/091043–14 $17.50

Received June 1996
Revised January 1997

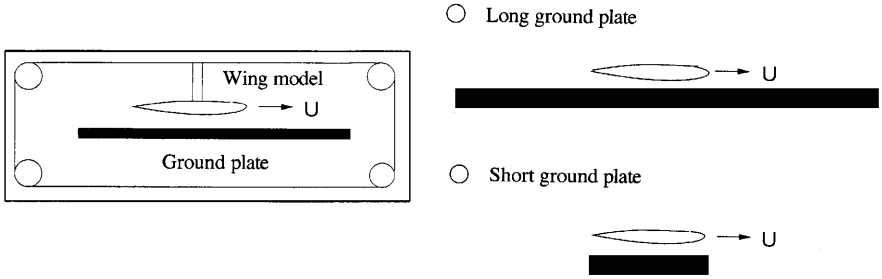

Figure 1. Experimental model for ground effect

adaptability to complicated configurations and its small scale of calculation. Above all, as a boundary element method, it has features such as consideration of the wing thickness effect, arbitrariness of the configuration in a range where linear approximation is adequate, option of angle of attack, etc. and is said to be an excellent method because of its versatility and facility in handling.

This work aims at determining the characteristics of the pressure variation produced when a wing model passes over a ground plate as illustrated in Figure 1. Analysis was made with two types of ground plates, i.e. a long one and a short one. The reason two types of ground plates are used is that the long one is to deal with a steady problem, whereas the short one is to deal with an unsteady problem in making numerical analysis. With the long ground plate Morino's method[6] was used. With the short ground plate the numerical method was expanded so as to allow Morino's method to deal with the relative motion. Experiments corresponding to the above were also conducted concurrently and a comparison of these experiments with the calculational results is made.

2. NUMERICAL CALCULATION METHOD

2.1. Calculations with long ground plate

If we assume the long ground plate as a finite ground, the pressure distribution which is formed around the wing in a uniform flow may be regarded as the pressure variation which is generated by a moving wing in a static fluid. Accordingly, the long ground plate can be used to deal with a steady problem. Supposing that the flow around the wing is incompressible, inviscid and irrotational, the velocity potential $\Phi(x, y, z)$ and disturbance velocity potential $\phi(x, y, z)$ are determined as shown below. Here it is assumed that the x-axis is taken in the direction conforming to the uniform flow $\mathbf{U}_\infty$.

$$\Phi = U_\infty(x + \phi). \tag{1}$$

The velocity potential Φ is related to the velocity $\mathbf{v}(x, y, z)$ of the flow by

$$\mathbf{v} = \text{grad } \Phi = \mathbf{U}_\infty + U_\infty \text{ grad } \phi. \tag{2}$$

Furthermore, the governing equation in the flow field is expressed by Laplace's equation shown below with respect to the disturbance velocity potential:[7]

$$\left(\frac{\partial^2}{\partial x^2} + \frac{\partial^2}{\partial y^2} + \frac{\partial^2}{\partial z^2}\right)\phi = 0. \tag{3}$$

As the boundary condition, the one shown below indicating that the flow moves along the body surfaces is used. In this paper the body surfaces include the surfaces of the wing, ground plate and sidewalls.

$$\frac{\partial \phi}{\partial n} = -\frac{\mathbf{U}_\infty \cdot \mathbf{n}}{U_\infty}, \tag{4}$$

where $\mathbf{n}$ is normal to the surface of the bodies.

In accordance with Morino's method,[6] let Green's theorem be applied to the surface S of the bodies. Taking a collocation point on the surface of the bodies and substituting the boundary condition for the formula gives the boundary integral equation

$$\begin{aligned} \tfrac{1}{2}\phi(P) - \frac{1}{4\pi} \iint\!\!\!\!\!\!\bigcirc_{S_B} \phi(Q) \frac{\partial}{\partial n(Q)} \frac{1}{r(P,Q)}\, \mathrm{d}S - \frac{1}{4\pi} \int\int_{S_W} \Delta\phi(Q) \frac{\partial}{\partial n(Q)} \frac{1}{r(P,Q)}\, \mathrm{d}S \\ = -\frac{1}{4\pi} \iint\!\!\!\!\!\!\bigcirc_{S_B} \frac{1}{r(P,Q)} \left(-\frac{\mathbf{U}_\infty \cdot \mathbf{n}}{U_\infty} \right) \mathrm{d}S, \end{aligned} \tag{5}$$

with

$$r(P,Q) = \sqrt{[(x-x_1)^2 + (y-y_1)^2 + (z-z_1)^2]},$$

where r represents the distance between the collocation point $P(x_1, y_1, z_1)$ and the integral point $Q(x, y, z)$. S_B is the surface of the bodies and S_W is that of the wake (Figure 2). We assume the wake surface to be a sheet of zero thickness and denote the intersection curve between S_B and S_W by C_W. We may take C_W to coincide with the trailing edge of the wing.[8] $\Delta\phi$ is the difference in the disturbance velocity potential across the wake. Let it be assumed that $\iint\!\!\!\!\!\!\bigcirc$ shows Cauchy's principal value of the integral. The above expression is a Fredholm integral equation of the second kind.

Although the influence of the wake has to be considered with a lifting body, the conditions that the potential difference $\Delta\phi$ between the upper and lower surfaces of the wake is constant along the streamline and that $\Delta\phi$ is equal to the value at the trailing edge of the wing are hereby imposed as Kutta's condition, since no pressure difference can exist in the wake:[9]

$$\Delta\phi = \phi_u - \phi_l = \text{const.}, \tag{6}$$

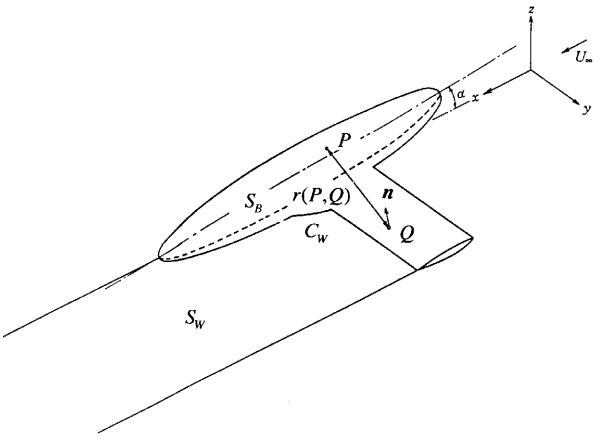

Figure 2. Formulation of model

where ϕ_u and ϕ_l are the values of ϕ on S_B at two points located just above and below a point belonging to C_W respectively, from which the stream under consideration is shed.

By solving this integral equation with the disturbance velocity potential ϕ as an unknown, the flow field can be obtained. In order to obtain an approximate solution for the integral equation, the surfaces S_B and S_W are divided into small quadrilateral panels S_k. The surface panels S_k are approximated by a hyperbolic paraboloid. The values of ϕ and $\partial\phi/\partial n$ are assumed to be constant within each panel. The collocation method is then used, i.e. equation (5) is satisfied at the centres $\mathbf{P}_h$ of the elements S_h. According to this method, the disturbance velocity potential ϕ is discretized to the degree of freedom to the extent of the division number N of the panel and we have the linear simultaneous equations

$$[\delta_{hk} - C_{hk} - W_{hk}]\{\phi_k\} = -[B_{hk}]\left\{-\frac{\mathbf{U}_\infty \cdot \mathbf{n}_k}{U_\infty}\right\}, \tag{7}$$

where δ_{hk} indicates Kronecker's delta and the aerodynamic influence coefficients C_{hk}, B_{hk} and W_{hk} are expressed as

$$C_{hk} = \left[\frac{1}{2\pi}\iint_{S_B} \frac{\partial}{\partial n}\left(\frac{1}{r}\right) \mathrm{d}S\right]_{P=P_h}, \quad B_{hk} = \left[\frac{1}{2\pi}\iint_{S_B} \frac{1}{r}\,\mathrm{d}S\right]_{P=P_h}, \quad W_{hk} = \left[\frac{\pm 1}{2\pi}\iint_{S_W} \frac{\partial}{\partial n}\left(\frac{1}{r}\right) \mathrm{d}S\right]_{P=P_h}. \tag{8}$$

The aerodynamic influence coefficients are analytically obtained by Morino *et al.*[6] Therefore no numerical integrals are used in obtaining C_{hk}, B_{hk} and W_{hk}.

The velocity can be obtained by differentiating the velocity potential. For the differential along the surface of the body, Yanagizawa's method[10] is employed. In order to obtain the velocity and pressure distribution, we approximate the velocity potential Φ by the parabolic distribution for steady flow:

$$\Phi = U_\infty(x + \phi) = as^2 + bs + c, \tag{9}$$

where s is the length along a circular arc through three consecutive collocation points and is measured from the centre collocation point. The constants a, b and c are calculated from the values of velocity potential at the three collocation points. We need derivatives of Φ with respect to s in two directions determined by a pair of three collocation points as

$$\frac{\mathrm{d}\Phi}{\mathrm{d}s_1} = \Phi_{s_1} = 2a_1 s_1 + b_1, \qquad \frac{\mathrm{d}\Phi}{\mathrm{d}s_2} = \Phi_{s_2} = 2a_2 s_2 + b_2, \tag{10}$$

where s_1 measured from $P_{i,j}$ is the length along the circular arc through points $P_{i-1,j}, P_{i,j}, P_{i+1,j}$ and s_2 measured from $P_{i,j}$ is the length along the circular arc through $P_{i,j-1}, P_{i,j}, P_{i,j+1}$ as shown in Figure 3.

We want to determine the unit tangential vectors $\mathbf{l}_1$ and $\mathbf{l}_2$ at the central collocation point $P_{i,j}$ along s_1 and s_2 respectively. As a special case, if the three consecutive collocation points lie on a straight line, the unit tangential vector $\mathbf{l}$ is simply given by

$$\mathbf{l} = \frac{\mathbf{b}}{|\mathbf{b}|}. \tag{11}$$

If this is not the case, $\mathbf{l}$ is determined according to the following scheme. We denote here by $\mathbf{r}_0$ the position vector of the centre of the circle through the three points $P_{i-1,j}, P_{i,j}, P_{i+1,j}$ and define the vectors $\mathbf{a}$, $\mathbf{b}$ and $\mathbf{c}$ as shown in Figure 3. With these preliminaries the vector $\mathbf{r}_0$ is calculated as

$$\mathbf{r}_0 = \mathbf{a} + s_c\mathbf{b} + t_c\mathbf{c}, \tag{12}$$

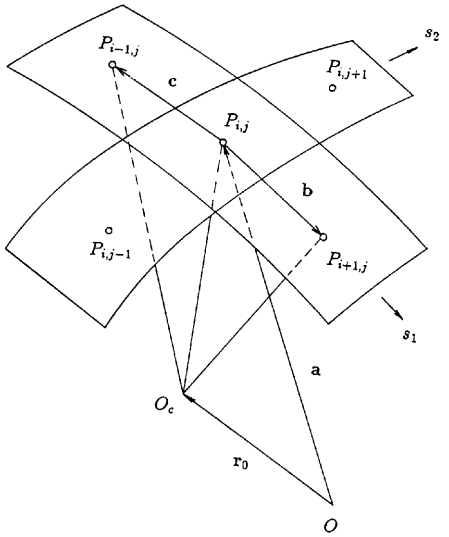

Figure 3. Derivatives along body surface

with

$$s_c = \frac{(\mathbf{b}^2 - \mathbf{b}\cdot\mathbf{c})\mathbf{c}^2}{2[\mathbf{b}^2\mathbf{c}^2 - (\mathbf{b}\cdot\mathbf{c})^2]}, \qquad t_c = \frac{(\mathbf{b}\cdot\mathbf{c} - \mathbf{c}^2)\mathbf{b}^2}{2[(\mathbf{b}\cdot\mathbf{c})^2 - \mathbf{b}^2\mathbf{c}^2]}. \tag{13}$$

Then the tangential vector is given by

$$\mathbf{l} = \mathbf{n}_n \times \mathbf{n}_r, \tag{14}$$

where

$$\mathbf{n}_n = \frac{\mathbf{b}\times\mathbf{c}}{|\mathbf{b}\times\mathbf{c}|}, \qquad \mathbf{n}_r = \frac{\mathbf{a}-\mathbf{r}_0}{|\mathbf{a}-\mathbf{r}_0|}. \tag{15}$$

The vector $\mathbf{n}_n$ is the unit normal vector of the plane determined by vectors $\mathbf{b}$ and $\mathbf{c}$, while the vector $\mathbf{n}_r$ is the unit vector along the radius of the circle through the point $P_{i,j}$. The symbol $(\cdot)$ denotes the inner product of vectors and the symbol $(\times)$ denotes the external product of vectors. In the directions of s_1 and s_2 we have

$$\mathbf{l}_1 = \frac{\mathbf{b}_1}{|\mathbf{b}_1|} \quad \text{and} \quad \mathbf{l}_2 = \frac{\mathbf{b}_2}{|\mathbf{b}_2|} \quad \text{along straight lines,} \tag{16}$$

$$\mathbf{l}_1 = \mathbf{n}_{n_1} \times \mathbf{n}_{r_1} \quad \text{and} \quad \mathbf{l}_2 = \mathbf{n}_{n_2} \times \mathbf{n}_{r_2} \quad \text{along curves.} \tag{17}$$

If we take the e_1-axis in the direction of s_1 and the e_2-axis in the direction perpendicular to e_1 and in the plane spanned by s_1 and s_2, then we have

$$\phi_{e_1} = \frac{\mathrm{d}\Phi}{\mathrm{d}e_1} = \frac{\mathrm{d}\Phi}{\mathrm{d}s_1}, \tag{18}$$

$$\phi_{e_2} = \frac{\mathrm{d}\phi}{\mathrm{d}e_2} = \frac{1}{\sqrt{[1-(\mathbf{l}_1\cdot\mathbf{l}_2)^2]}}\left(\frac{\mathrm{d}\Phi}{\mathrm{d}s_2} - (\mathbf{l}_1\cdot\mathbf{l}_2)\frac{\mathrm{d}\Phi}{\mathrm{d}s_1}\right). \tag{19}$$

Then the pressure coefficient and velocity vector are expressed as

$$\nabla\Phi \cdot \nabla\Phi = \Phi_{e_1}^2 + \Phi_{e_2}^2, \tag{20}$$

$$C_{\mathrm{p}} = \frac{p - p_\infty}{\frac{1}{2}\rho U_\infty^2} = 1 - \frac{\Phi_{e_1}^2 + \Phi_{e_2}^2}{U_\infty^2}, \tag{21}$$

$$\mathbf{v} = \Phi_{e_1}\mathbf{l}_1 + \Phi_{e_2}\frac{\mathbf{l}_2 - (\mathbf{l}_1 \cdot \mathbf{l}_2)\mathbf{l}_1}{\sqrt{[1 - (\mathbf{l}_1 \cdot \mathbf{l}_2)^2]}}. \tag{22}$$

2.2. *Calculations with short ground plate*

We consider mainly the pressure variation on the short ground above which the wing passes. In this case the phenomenon of the aerodynamic forces surrounding the wing and short plate is a relative motion in a fluid at rest in three dimensions and the matter has to be dealt with as an unsteady problem.

The steady flow of a fluid past a body has been investigated by many authors, but there have been few works on the unsteady flow due to several bodies in relative motion. Some features of the flow make the study difficult. The boundary configuration of the flow field changes with time. The boundary element method is used to remove the difficulties in this research. There is no need to regenerate the panel at each time step unless the moving bodies change their shape. This is a great advantage of the boundary element method and shortens the turnaround time in parametric studies. The boundary element method is modified to treat the unsteady aerodynamic phenomena. To avoid overlapping the description, only the factors different from the long ground plate, i.e. the boundary condition, differential of the velocity potential and calculation of the pressure field, are referred to.

We shall consider the case where the wing is passing over the short ground at rest. Here it is assumed that the x-axis is parallel to the direction of the velocity of the wing. The instant just when the wing comes over the short ground plate as in Figure 1 is chosen as the origin of time ($t = 0$). The problem is solved as an initial value problem. At each time interval a boundary value problem is solved for the velocity potential outside the bodies.

In this case with the short ground plate the velocity potential is related to the velocity of the flow by

$$\mathbf{v} = u_{\mathrm{w}} \operatorname{grad} \phi, \tag{23}$$

where the value of u_{w} is the largest velocity of the bodies. The boundary condition is given as

$$\frac{\partial\phi}{\partial n} = \frac{\mathbf{u}_{\mathrm{w}} \cdot \mathbf{n}}{u_{\mathrm{w}}}, \tag{24}$$

where $\mathbf{u}_{\mathrm{w}}$ is the velocity of the body surfaces.

The velocity is evaluated by taking the gradient of equation (5):

$$E(P)\mathbf{v}(P) - \frac{1}{4\pi}\oiint_{S_{\mathrm{B}}} \phi(Q)\nabla_P \frac{\partial}{\partial n(Q)}\frac{1}{r(P,Q)}\,\mathrm{d}S - \frac{1}{4\pi}\iint_{S_{\mathrm{W}}} \Delta\phi(Q)\nabla_P \frac{\partial}{\partial n(Q)}\frac{1}{r(P,Q)}\,\mathrm{d}S$$
$$= -\frac{1}{4\pi}\oiint_{S_{\mathrm{B}}} \frac{\partial\phi}{\partial n}\nabla_P \frac{1}{r(P,Q)}\,\mathrm{d}S. \tag{25}$$

Equation (25) is approximated in accordance with Suciu's method[11] as

$$2E_h\mathbf{v}_h = \sum_k \phi_k \nabla_P C_{hk} - \sum_k \left(\frac{\partial\phi}{\partial n}\right)_k \nabla_P B_{hk} + \sum_k \Delta\phi_k \nabla_P W_{hk}, \tag{26}$$

where C_{hk}, B_{hk} and W_{hk} are given by equations (7) or

$$E_h = \begin{cases} 1 & \text{outside } S_h, \\ \frac{1}{2} & \text{on } S_h, \\ 0 & \text{inside } S_h, \end{cases} \tag{27}$$

$$\nabla_P C_{hk} = \left[\frac{1}{2\pi} \iint_{S_B} \nabla_P \frac{\partial}{\partial n} \left(\frac{1}{r} \right) \mathrm{d}S \right]_{P=P_h}, \qquad \nabla_P B_{hk} = \left[\frac{-1}{2\pi} \iint_{S_B} \nabla_P \frac{1}{r} \, \mathrm{d}S \right]_{P=P_h},$$
$$\nabla_P W_{hk} = \left[\frac{\pm 1}{2\pi} \iint_{S_W} \nabla_P \frac{\partial}{\partial n} \left(\frac{1}{r} \right) \mathrm{d}S \right]_{P=P_h} \tag{28}$$

and ∇_P is the gradient at collocation point P.

The gradient of the aerodynamic influence coefficients is analytically obtained by Suciu and Morino.[11] Therefore no numerical integrals are used in obtaining $\nabla_P C_{hk}, \nabla_P B_{hk}$ and $\nabla_P W_{hk}$.

The pressure on the surface of the bodies can be obtained from an extension of Bernoulli's theorem. The pressure coefficient may be written as

$$C_P = -\frac{2\partial\phi/\partial t}{u_w^2} - \frac{|\mathbf{v}|^2}{u_w^2}. \tag{29}$$

Through the first term on the right-hand side we include unsteadiness. Evaluation of this term is not easy, because it includes the partial derivative of the velocity potential with respect to time. When we calculate the time differentiation, we have to consider that the bodies move relative to each other. In this connection a number of methods to obtain the time differential term of the disturbance velocity have been proposed.[12,13] In this study we evaluate the term as[14]

$$2E_h \frac{\partial \phi_h}{\partial t} = -\sum_k (\vec{\nabla}_P C_{hk} + \vec{\nabla}_P \bar{W}_{hk}) \cdot \vec{u}_k \phi_k + \sum_k \vec{\nabla}_P B_{hk} \cdot \vec{u}_k \left(\frac{\partial \phi}{\partial n} \right)_k - \sum_k (C_{hk} + \bar{W}_{hk}) \frac{\partial \phi_k}{\partial t}. \tag{30}$$

In Reference 14 we do not consider the effect of the wake. In equation (30) the terms including $\bar{W}_{hk}$ and $\vec{\nabla}_P \bar{W}_{hk}$ on the right-hand side are newly added to include the influence of the wake. Using this equation, we can get accurate results and shorten the calculation time.

3. ANALYTICAL RESULTS

3.1. Long ground plate

The wing section used for the calculation is NACA65A010. The size of the analytical model is given as illustrated in Figure 4 by taking the length in the uniform flow direction as $10c$, the length in

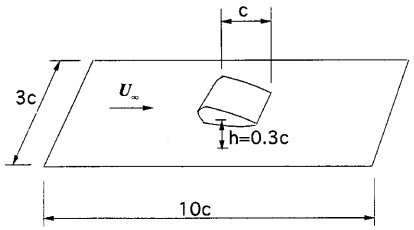

Figure 4. Model dimensions in case of long ground plate

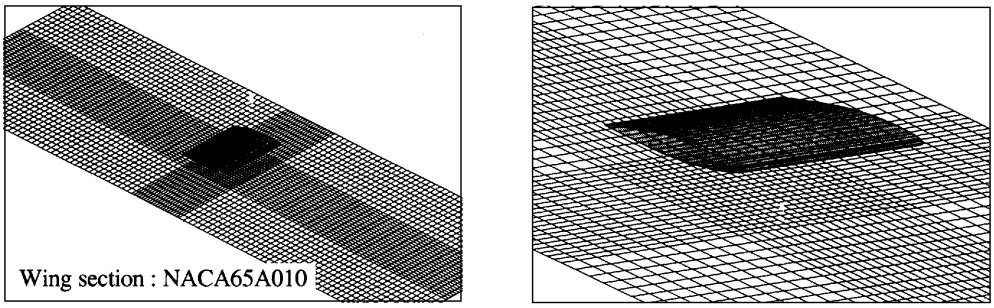

Figure 5. Numerical model in case of long ground plate: left, whole view; right, expanded view

the direction perpendicular to the said direction as $3c$ and the height of the wing from the ground plate as $0{\cdot}3c$ on the assumption that the chord length is c. The numerical model is depicted in Figure 5.

The time variation of the pressure produced on the ground when the wing passes over it is shown in Figure 6. First, positive pressure is generated as the leading edge of the wing passes. After that, negative pressure which is greater in absolute value is generated and positive pressure is again seen when the trailing edge of the wing passes. With regard to the positive/negative peak values, the positive pressure part becomes greater and the negative pressure part becomes smaller as the angle of attack is increased. These tendencies are likewise noted when the angle of attack is steered negative. The result brought about when the angle of attack is steered negative will be omitted for lack of space. Comparison of the calculational result with the experimental result clarifies the tendency that the calculational result closely follows the experimental result, despite the fact that the absolute values are slightly different from each other.

The results of frequency analysis of the wave-form of the pressure variation when the wing passes are shown in Figure 7. From the calculational result a peak is seen in the vicinity of approximately 5–6 Hz. Furthermore, the peak is transferred to the high-frequency side upon increasing the angle of attack. It is observed from the experimental result that the data at the angle of attack 0° cannot be obtained so well, but the features seen with the calculational result are expressed also with the experimental result.

Next, the pressure distribution on the ground plate is mapped in Figure 8. At the angle of attack 0° it is noticed that positive pressure is generated on the leading and trailing edges of the wing. It is also seen that negative pressure is produced underneath the wing. As the angle of attack is increased, the

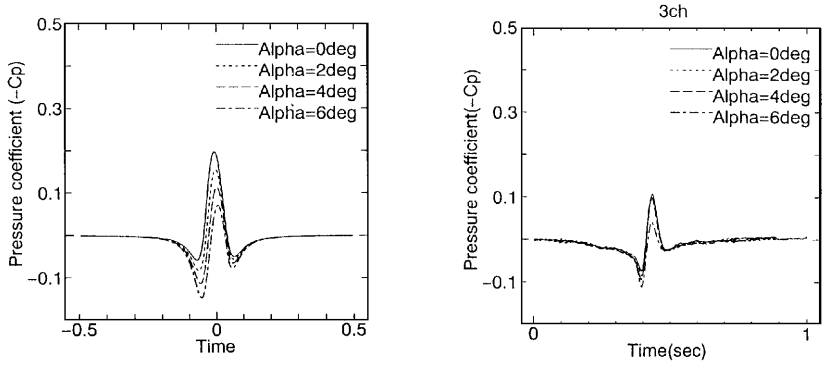

Figure 6. Time variation of pressure generated on ground plate when wing passes over: left, calculation; right, experiment

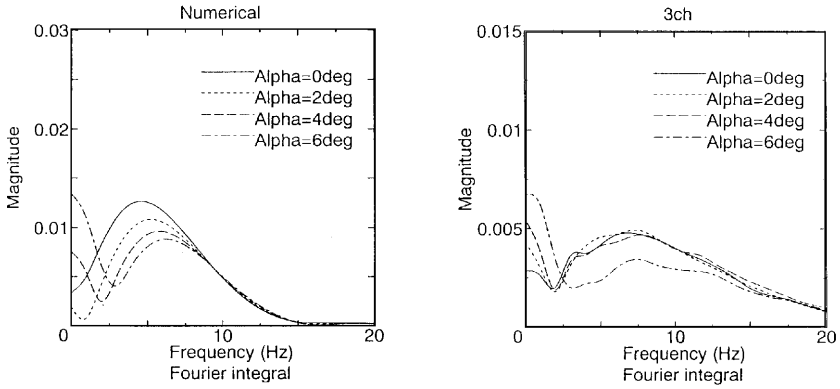

Figure 7. Frequency analysis of pressure variation when wing passes over: left, calculation; right, experiment

region of positive pressure increases and the region of negative pressure becomes smaller. On the other hand, two streaks of negative pressure presumably caused by the trailing vortex appear at the rear side of the wing at the angle of attack 6°.

It is exceedingly difficult to measure the pressure on the surface of the moving wing by experiments, but numerical calculations facilitate the measurements. Figure 9 show the pressure distribution on the wing root. For the angle of attack 0° a symmetric pressure distribution on both the upper and lower sides of the wing is given provided that the ground plate is not under the wing, because the wing section used is symmetric. In contrast, with the negative pressure underneath the wing becomes greater when the ground plate is available and in this case the pressure distribution is not symmetric on either the upper or the lower side. As the angle of attack is gradually increased, the negative pressure on the upper side and the positive pressure on the lower side becomes greater, as can be seen at the angle of attack 6°. Thus it is imagined that the lift force as a whole is increased.

Looking at Figure 10, we see that the features described above more plainly. It turns out that the presence of the ground plate allows the gradient of the lift force coefficient to be heightened.

Analysis so far has been made exclusively with the ground plate without considering a sidewall in the calculation. On the other hand, the experiment was also carried out using an apparatus with a sidewall. Thus calculation was made with respect to the numerical model mapped in Figure 11, with the aim of ascertaining how the pressure distribution is changed by the influence of the sidewall. The

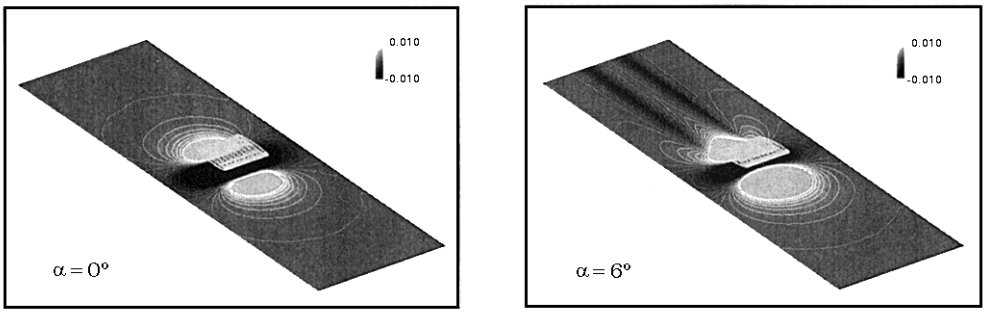

Figure 8. Pressure distribution on ground plate

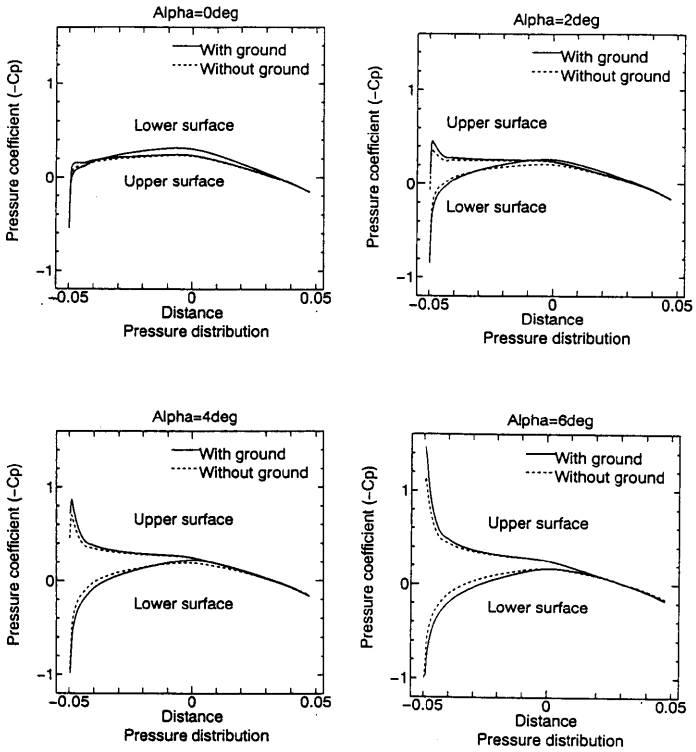

Figure 9. Pressure distribution on wing

pressure distribution of both the ground plate and the sidewall is shown in Figure 12. However, for the sake of observation, the sidewall in the foreground (see Figure 11) is omitted.

The pressure distribution on the sidewall seen in Figure 12 appears hardly to influence the pressure variation on the centreline of the ground plate, as shown in Figure 13. Therefore, as far as the pressure variation on the centreline of the ground plate is concerned, it is believed that analysis might be made without considering the sidewall.

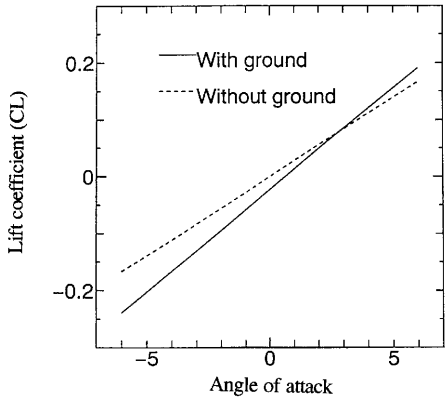

Figure 10. Lift coefficient

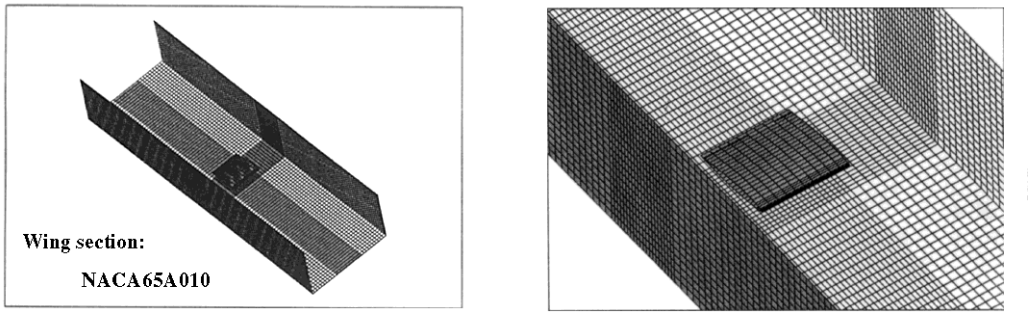

Figure 11. Numerical model when sidewalls are considered: left, whole view; right, expanded view

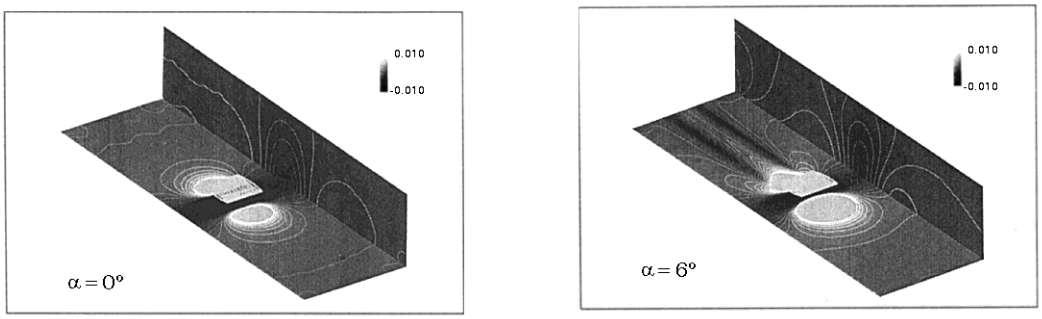

Figure 12. Pressure distribution on ground plate and sidewall

3.2. *Short ground plate*

The wing section used is NACA65A010, the same as that for the long ground plate. The size of the analytical model is given in Figure 14. On the assumption that the chord length is c, it is determined that the length of the ground plate in the transfer direction is c, the length perpendicular to the former is $3c$ and the height of the wing from the ground plate is $0{\cdot}3c$.

The numerical model is mapped in Figure 15. Although the short ground plate brings forth an unsteady problem, the time interval used for the calculation was determined to be $t = c/u_w = 0{\cdot}01$ in

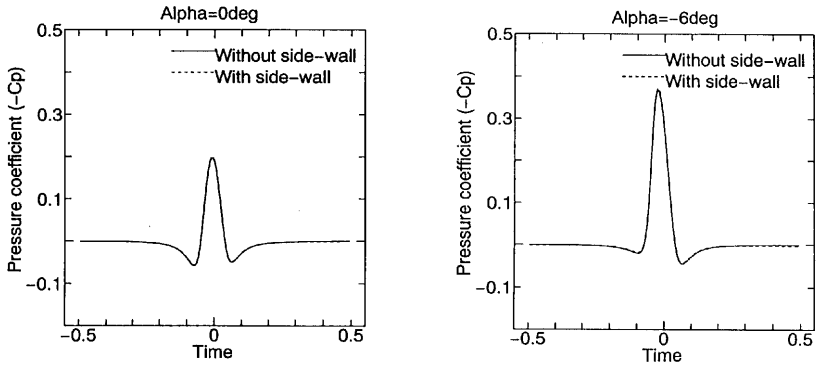

Figure 13. Pressure variation on ground plate when sidewall is considered

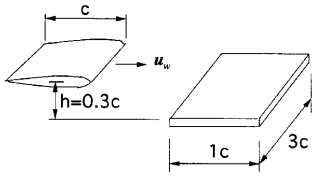

Figure 14. Model dimensions in case of short ground plate

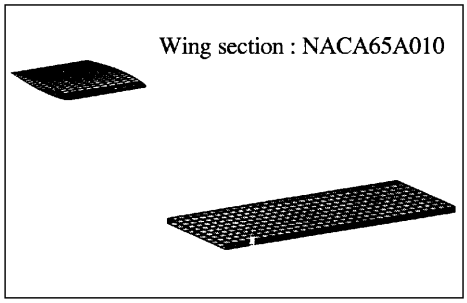

Figure 15. Numerical model in case of short ground plate

dimensionless time. The calculation time was determined to be between $-0{\cdot}4$ and $0{\cdot}4$. We assume the velocity of the body surfaces as

$$u_{\mathrm{w}} = \begin{cases} 1 & \text{on the wing,} \\ 0 & \text{on the ground plate.} \end{cases}$$

The time variation of the pressure generated on the ground when the wing passes over it is shown in Figure 16. The tendency of the wave-form is almost the same as that seen with the long ground plate. As the experimental value to be compared, only the value at the time when the angle of attack is 0° is available, owing to restriction on use of the experimental apparatus. However, it is considered that the calculational value fits the experimental value very well.

With the long ground plate there always exists a ground plate on the lower side of the wing, as viewed from the wing, and the left force applied to the wing is time-dependently constant. On the other hand, with the short ground plate at first there is no ground plate, then the ground plate appears

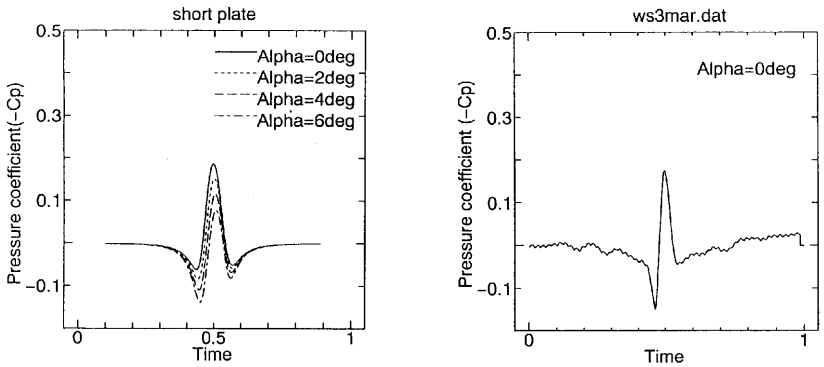

Figure 16. Time variation of pressure generated on ground plate when wing passes over: left, calculation; right, experiment

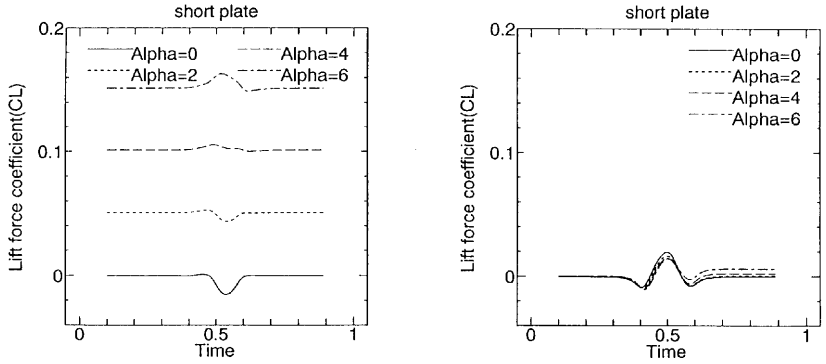

Figure 17. Time variation of lift coefficient: left, lift applied to wing; right, lift applied to ground plate

and again disappears. This should be called intrinsically unsteady phenomenon. For this reason the lift force applied both to the wing and to the ground plate also varies time-dependently, as shown in Figure 17. Although the lift force generated by the angle of attack is applied to the wing at first, it is discerned how the said lift force is changed owing to the influence of the ground plate when the wing passes over it.

When the wing passes over the ground plate, the tendency of the graph of the lift force coefficient is reversed owing to the difference in the angle of attack (from $\alpha = 2^\circ$ to 4°). This might be caused by the following. When the angle of attack is small enough, the flow route on the lower side of the wing is made narrower and the negative pressure is increased with an increased flow velocity, allowing the lift force coefficient to decrease. On the other hand, when the angle of attack is large, the flow is intercepted to increase the positive pressure. Thus the lift force coefficient is increased.

The tendency in the graph of the lift force coefficient is reversed owing to the difference in attack, for the reason which can also be explained from Figure 10. That is to say, when the angle of attack is smaller than approximately 3°, with this as a limit, the lift force coefficient with the ground plate becomes smaller than that without the ground plate. In contrast, when the said angle is larger, the lift force coefficient increases. On the other hand, the lift force applied to the ground plate also changes when the wing passes over it.

4. CONCLUSIONS

The pressure variation produced when a wing passes over a ground plate has been analysed with respect to both long and short ground plates using the boundary element method. The calculational results have been found to be in good qualitative agreement with the experimental values. It is made clear as a result that evaluation is possible with the pressure variation generated by the passing wing in accordance with the steady boundary element method with a long ground plate and in accordance with the unsteady boundary element method with a short ground plate.

REFERENCES

1. C. Wieseelsberger, 'Wing resistance near the ground', *NACA TM77*, 1922.
2. M. P. Fink and J. L. Lastinger, 'Aerodynamic characteristics of low-aspect-ratio wings in close proximity to the ground', *NASA TN-D926*, 1961.
3. A. Plotkin and C. G. Kennell, 'Thickness-induced lift on a thin airfoil in ground effect', *AIAA J.*, **19**, (1981).

4. H. Tomaru and Y. Kohama, 'Wind-tunnel investigation of aerofoil for wing in ground effect', *J. Jpn. Soc. Fluid Mech.*, **10**, 47–60 (1991) (in Japanese).
5. S. Ando, 'Note on prediction method of aerodynamic performance of WIG at cruise', *J. Jpn. Soc. Aeronaut. Space Sci.*, **42**, 483–493 (1994).
6. L. Morino, L. T. Chen and E. O. Suciu, 'Steady and oscillating subsonic and supersonic aerodynamics around complex configurations', *AIAA J.*, **13**, 368–374 (1975).
7. J. Katz and A. Plotkin, *Low-Speed Aerodynamics*, McGraw-Hill, New York, 1991.
8. M. Yanagizawa, 'A study of steady and unsteady aerodynamic characteristics on a 3-D lifting body in subsonic flow using boundary element method', *Doctoral Thesis*, University of Tokyo, 1985 (in Japanese).
9. L. Morino, 'A general theory of unsteady compressible potential aerodynamics', *NASA CR-2464*, 1974.
10. M. Yanagizawa and K. Kikuchi, 'Finite element calculations for aerodynamic coefficients of 3-dimensional body in subsonic flow using Green's function method', *National Aerospace Laboratory TR-724*, 1976 (in Japanese).
11. E. O. Suciu and L. Morino, 'A nonlinear finite element analysis of wings in steady incompressible flows with wake roll-up', *AIAA Paper 76–64*, 1976.
12. K. Ashihara, E. Morishita and H. Koyama, 'A study on the unsteady ground-effect', *Proc. 26th Fluid Dynamics Conf.*, the Japan Society for Aeronautical and Space Sciences, Japan Society of Fluid Mechanics, Fukuoka, 1994, pp. 341–344 (in Japanese).
13. T. Mojima, H. Takase, K. Sakai, E. Shima and T. Handa, 'Application of aerodynamic analysis technology to train shape design', *Kawasaki Tech. Rev.*, **126**, 38–43 (1995) (in Japanese).
14. K. Kikuchi, T. Maeda and M. Yanagizawa, 'Numerical simulation of the phenomena due to the passing-by of two bodies using the unsteady boundary element method', *Int. j. numer. methods fluids*, **23**, 445–454 (1996).

